Maternal microbiota *Bifidobacterium* promotes placental morphogenesis, nutrient transport and fetal growth in mice

Authors: Jorge Lopez-Tello[1]*, Zoe Schofield[2]*, Raymond Kiu[2], Matthew J. Dalby[2], Douwe van Sinderen[3], Gwénaëlle Le Gall[4], Amanda N Sferruzzi-Perri[1†], Lindsay J Hall[2,5†]

Affiliations:
[1]Department of Physiology, Development, and Neuroscience, Centre for Trophoblast Research, University of Cambridge, Cambridge, UK
[2]Gut Microbes & Health, Quadram Institute Bioscience, Norwich Research Park, Norwich, UK
[3]APC Microbiome Institute, University College Cork, Cork, Ireland
[4]Norwich Medical School, University of East Anglia, Bob Champion Research and Education Building, James Watson Road, Norwich Research Park, Norwich NR4 7UQ, UK
[5]Chair of Intestinal Microbiome, School of Life Sciences, ZIEL – Institute for Food & Health, Technical University of Munich, Freising, Germany

[*†]Contributed equally

Corresponding author names:
Jorge Lopez-Tello (jl898@cam.ac.uk)
Amanda N. Sferruzzi-Perrri (ans48@cam.ac.uk)
Lindsay J Hall (Lindsay.Hall@tum.de **I** Lindsay.Hall@quadram.ac.uk)

Author Contributions: JL-T, ZS, ANS-P, LJH designed research; JL-T, ZS, RK, GLG conducted research, JL-T, ZS, RK, MJD contributed analytic tools and performed analysis; DvS contributed reagents; JL-T, ZS, ANS-P, LJH wrote the paper with feedback from all the authors.

Competing Interest Statement: The authors declare that they have no competing interests.

Classification: Biological Sciences – Physiology

Keywords: Pregnancy, Placenta, Microbiota, Fetus, *Bifidobacterium*

This file includes:

Main Text: 5,454 (introduction, results, discussion and methods)
Main Figures: 3
Tables: 1
Supplementary Figures: 4

Supplementary Tables: 3
References: 55

Significance: Metabolism is highly influenced by the gut microbiota, which is particularly important during gestation, when key metabolites are used for feto-placental growth. However, the contribution of the maternal gut microbiota (and microbiota-generated metabolites) in determining fetal outcomes is largely unexplored. Here, we show that maternal gut communities and specific microbiota members are key modulators of placental phenotype with important consequences for fetal development. We have revealed novel roles for a maternal *Bifidobacterium* strain, that include the control of placental capillary morphogenesis and nutrient transporters (glucose and lipids), which affect fetal metabolism and growth. Our work has important implications for the establishment of novel therapeutic strategies to treat pregnancy complications.

Abstract

The gut microbiota plays a central role in regulating host metabolism. However, while substantial progress has been made in discerning how the microbiota influences host functions post birth and beyond, little is known about how key members of the maternal gut microbiota can influence feto-placental growth. Here, using germ-free and specific-pathogen-free mice, we demonstrate that the bacterium *Bifidobacterium breve* UCC2003 modulates maternal body adaptations, placental structure and nutrient transporter capacity, with implications for fetal metabolism and growth. The effects of *B. breve* UCC2003 on feto-placental growth are mediated, in part, by changes in the maternal and placental metabolome (*i.e.* acetate and carnitine). Histological analysis of the placenta confirmed that *Bifidobacterium* modifies placental structure via changes in *Igf2P0, Dlk1, Mapk1* and *Mapk14* expression. Additionally, *B. breve* UCC2003, acting through *Slc2a1* and *Fatp3-4* transporters, was shown to restore fetal glycaemia and fetal growth in association with changes in the fetal hepatic transcriptome. This study provides knowledge towards a novel and safe therapeutic strategy for treating pregnancy disorders via modulation of the maternal gut microbiota.

Main Text

Introduction

All nutrients and metabolites required for feto-placental growth are provided by the mother, which in turn is thought to be influenced by the maternal gut microbiota through breakdown of complex dietary components (1). During gestation, liberated metabolites may be used by the placenta for morphogenesis, and transported across the placenta for use by the fetus for growth and development (2, 3). This is highly important across gestation, particularly at later stages, when fetal growth is maximal. Notably, there are also alterations in the maternal microbiota throughout pregnancy with levels of the beneficial bacterial genus *Bifidobacterium*

rising from trimester 1 onwards (4–6). Failure of the mother to provide nutrients and metabolites to the fetus can result in pregnancy complications including small for gestational age (SGA), fetal loss and stillbirth. However, the contribution of the maternal microbiota in determining fetal outcomes is largely unexplored. Knowledge in this area would be highly valuable for developing treatments to improve fetal growth, with benefits for population health.

Studies performed with Germ free (GF) mice have identified that the microbiota is a key regulator for adequate development, early immune education and metabolism (7–11). However, little is known about how maternal microbiota influences feto-placental growth and more specifically, placental structure and function. Here, we hypothesized that the maternal gut microbiota, and specific microbiota members, regulate fetal growth by modulating placental development and nutrient supply. We tested this hypothesis by comparing conceptus growth in three different maternal gut microbiota conditions by using conventional specific-pathogen-free (SPF) mice (used as a base line to define correct feto-placental growth) (11), GF mice, and maternal GF mice colonized with *Bifidobacterium breve* UCC2003 (12). As a keystone microbiota member and 'probiotic' species, *B. breve* may represent a suitable option for treating pregnancy complications by exerting beneficial metabolic effects on maternal physiology and associated feto-placental growth. Indeed, *B. breve* induced changes in maternal physiology, placental morphogenesis and the abundance of placental glucose and lipid transporters, which were associated with improvements in growth and metabolism of the fetus.

Results

Germ-free mice treated with B. breve have altered body composition and caecum metabolic profile

To assess whether maternal microbiota is able to influence feto-placental growth, GF mice were treated orally with *B. breve* UCC2003 from day 10 of gestation (treatment on days 10, 12 and 14; i.e. BIF group), and compared to GF and SPF dams (for experimental overview see Figure S1). Timing and dosing were based on the fact that levels of *Bifidobacterium* rise throughout pregnancy (5) (colonization levels during pregnancy can be found in Figure S2). Moreover, previous work has indicated three consecutive doses of *B. breve* UCC2003 facilitates stable gut colonization, with the advantage of also avoiding repeated handling of the mice, which may induce spontaneous abortions (13, 14). In addition, from a translational point of view, we also wanted to correlate with potential future supplementation studies in women at the point pregnancy is confirmed.

Maternal body composition differed between groups with GF and BIF mice showing increased digestive tract weight and lower pancreas mass compared to SPF mice. GF and BIF mice had similar circulating concentrations of glucose and insulin to SPF mice (assessed in fed

118 conditions; Table 1). Compared to SPF mice, treatment with *B. breve* reduced maternal
119 gonadal fat depot, liver, and spleen weights in BIF mice. No differences were observed in the
120 circulating concentrations of leptin, cholesterol, triglycerides, or free fatty acids in maternal
121 serum (Table 1).
122
123 Metabolomics analysis in maternal caecum samples indicated that the concentration of 13 out
124 of 115 metabolites were significantly altered (Table 1 and Table S1). Acetate was significantly
125 influenced by *B. breve* (Table 1), with BIF dams having intermediate concentrations compared
126 to SPF and GF mice (the low levels of acetate detectable in GF mice, most likely originated
127 from the diet and/or are host-derived). These findings suggest that acetate producing *B. breve*
128 and the wider gut microbiota may exert selective effects on maternal metabolic (gonadal fat
129 depot and liver) and immune organs (spleen).
130
131 ***Maternal gut microbiota and B. breve regulate fetal growth by controlling fetal***
132 ***glycaemia***
133 Although the three experimental groups had similar numbers of viable fetuses per litter, the GF
134 group had higher numbers of resorptions within the litter (defined as large or small
135 hemorrhagic-to-black implantation sites) compared to SPF and BIF mice (Figure 1A-B).
136 Similarly, when this parameter was calculated as resorption rate, and corrected for litter size,
137 we found similar results (Figure S3). In fact, all GF dams had at least one resorption, whilst *B.*
138 *breve* reduced the appearance of resorptions by 50% (Figure 1B). No evidence of intrauterine
139 death, defined as a lack of fetal vascular flow in the yolk sac vessels, were found. Compared to
140 SPF and BIF mice, GF fetuses were growth restricted, hypoglycaemic and had reduced liver
141 weight, but had preserved brain size (Figure 1C-E). These findings highlight that the maternal
142 microbiota influence fetus viability and that *B. breve* is a strong modulator of fetal growth and
143 metabolism.
144
145 ***Maternal B. breve modulates fetal hepatic transcriptome***
146 The liver is a key organ for glucose storage and production. As fetuses from BIF mice had
147 enlarged livers and improved glycaemia, we next determined if there were changes in the fetal
148 hepatic transcriptome (livers were collected on GD18.5, when fetal liver function is particularly
149 active prior to term; Figure 1F). A total of 602 genes were differentially expressed, with 94
150 significantly up-regulated and 508 down-regulated genes in BIF group, when compared to GF
151 group (Figure 1G-H). Functional enrichment analysis indicated many metabolic pathways were
152 regulated in the fetal livers of BIF mice including carboxylic acid and lipid metabolic processes,
153 steroid hydroxylase activity, fatty acid metabolism and response to glucocorticoid (Figure 1I;
154 Table S2). Therefore, maternal *B. breve* appears to exert beneficial alterations in fetal hepatic
155 function to support fetal growth.
156

157 ***Maternal gut microbiota and B. breve control placental morphogenesis***
158 To further understand the links between the maternal microbiota and the regulation of fetal
159 growth, we assessed placental structure. When compared to SPF mice, placentas were lighter
160 in GF and BIF mice (Figure 2A). Placental efficiency, defined as the grams of fetus produced
161 per gram of placenta, was significantly improved in the BIF group compared to SPF and GF
162 mice (Figure 2B). Analysis of placental compartments showed that lack of maternal gut
163 microbiota significantly hampered growth of the placental labyrinth transport zone (Lz), without
164 compromising the endocrine junctional zone or decidua volumes (Figure 2C). It also did not
165 affect placental glycogen storage (Figure 2D) or the volume of the trophoblast (Figure E-F).
166 Analysis of maternal blood spaces revealed that the BIF group had reduced spaces compared
167 to SPF mice, while the volume and the length of fetal capillaries were significantly reduced in
168 the GF compared to SPF (Figure 2F-G). Similarly, surface area for exchange of the Lz was
169 significantly decreased in GF compared to SPF mice (Figure 2H). The barrier between
170 maternal and fetal blood was also determined to be thinner in BIF *versus* GF mice (Figure 2I).
171 Lz apoptosis levels were similar between groups (Figure 2J).
172
173 To define the molecular mechanisms behind the changes in the Lz, we quantified the
174 expression of select genes in micro-dissected Lz. Common angiogenic factors *Vegf, Ang1,*
175 *Ang2* were similarly expressed between groups (Figure 2K). However, the expression of
176 signaling pathways involved in cell proliferation and growth, namely the MAPK pathway, was
177 significantly altered by changes in maternal gut microbiota; *Mapk1* was shown to be increased
178 in both GF and BIF, while *Mapk14* (also known as *p38Mapk*) was revealed to be specifically
179 up-regulated in the Lz of BIF mice. In addition, *Dlk1* and *Igf2P0*, which are key genes
180 implicated in metabolism and Lz formation, were significantly up-regulated in the BIF group
181 compared to GF mice. The expression of *Akt* did not vary with group (Figure 2K). As informed
182 by western blotting, activation of ERK was reduced in the placental Lz of GF compared to SPF
183 mice, and this effect was reversed by BIF (Figure 2L). p38MAPK protein activity was similar
184 between groups. DLK1 protein level was also lower in GF compared to SPF mice. However
185 BIF increased DLK1 protein levels when compared to both SPF and GF mice (Figure 2L).
186 Further analysis by qPCR showed that the mRNA levels of *Nras*, but not *Kras*, were
187 significantly elevated in the BIF compared to the SPF group (Figure 2M). Overall, these
188 findings suggest that the maternal gut microbiota, and *B. breve*, regulate the development of
189 the mouse placental Lz via modulation of specific cell growth and metabolic genes/pathways.
190
191 ***Maternal gut microbiota and B. breve affect placental glucocorticoid handling and***
192 ***controls key placental nutrient transporters***
193 Glucocorticoids are a class of steroid hormones that can affect both fetal and placental
194 formation. To control glucocorticoid actions on the conceptus, the placenta expresses 11β-
195 hydroxysteroid dehydrogenase type 1 and 2 (*11Hsd1* and *11Hsd2*). We found that the

196 expression of *11Hsd1* was significantly elevated in the BIF group compared to the GF (no
197 change in *11Hsd2*; Figure 2N). Moreover, to better understand the changes in fetal growth and
198 glycemia between groups, we quantified the expression of selected amino acid, glucose and
199 lipid transporters in the Lz. We found no difference in the expression of system A amino acid
200 transporters (*Slc38a1, Slc38a2, Slc38a4*) between groups (Figure 2O). However, the key
201 glucose transporter *Slc2a1* was up-regulated in the Lz of BIF mice compared to GF mice
202 (*Slc2a3* mRNA levels were similar between groups; Figure 2O). Fatty acid transporters were
203 also altered, with high expression levels of *Fatp1* in the GF *versus* the SPF group, and
204 increased levels of *Fatp3* and *Fatp4* in the BIF group compared to the GF (Figure 2O; *Cd36*
205 expression levels were unaltered). Collectively, these data suggest that maternal gut
206 microbiota, and *B. breve*, regulate fetal growth by inducing changes in the expression of key
207 nutrient transporters within the placenta.
208
209 ***Differences in placental labyrinth growth are linked to an altered placental metabolome***
210 To gain further mechanistic understanding of the changes observed in the placental Lz and
211 fetal liver, we analysed >80 metabolites at GD16.5 (Figure 3 and Table S1). We found 5
212 metabolites significantly altered in the placental Lz (Figure 3). Aminoadipic acid in the Lz was
213 very low in GF/BIF groups as well as in fetal livers (Figure 3A). Treatment with *B. breve*
214 significantly reduced the concentrations of acetylcarnitine and carnitine in Lz tissue compared
215 to SPF placentas, but not in fetal livers (Figure 3B-C). Levels of formate in placental Lz were
216 significantly elevated in both GF and BIF compared to SPF mice (Figure 3D), with a similar
217 trend (although not significant) in fetal liver samples. Acetate was also altered in the Lz (Figure
218 3E), with concentrations significantly lower in the SPF compared to the GF group, whilst BIF
219 samples showed intermediate levels (although these levels were much lower than observed in
220 the maternal caecum). Similar to formate, concentrations of acetate in fetal liver followed
221 similar directions to the Lz, yet were not statistically different between groups. These data
222 suggest that maternal gut microbiota, and *B. breve*, regulate the fetal and placental growth via
223 modulation of the placental Lz metabolome.
224
225 **Discussion**
226 In this study, we provide evidence that the maternal microbiota and the microbiota member *B.*
227 *breve* regulate maternal body composition during gestation and beneficially modulate feto-
228 placental growth. To the best of our knowledge, this is the first demonstration of a maternal gut
229 bacterium remotely controlling placental structure and nutrient transporters, with important
230 implications for fetal glycaemia and fetal growth. We observed that the effects of
231 *Bifidobacterium* are partially mediated by altered metabolites in maternal caecum and in
232 placental Lz tissue, with alterations in the expression of key genes in the placental Lz and fetal
233 liver.
234

235 *Bifidobacterium* is the dominant microbiota member in vaginally delivered, breast fed infants,
236 with certain species and strains known to stimulate and aid the maturation of the immune
237 system (15). *B. breve* UCC2003 also regulates responses at the gut barrier, inducing
238 homeostatic epithelial cell programming, and protecting against inflammatory insults (14, 16).
239 Importantly, pregnancy is accompanied by increasing *Bifidobacterium* abundance in the gut of
240 women and mice (5), which is associated with changes in progesterone concentrations during
241 pregnancy. Additionally, alterations in the abundance of *Bifidobacterium* are also linked to the
242 development of serious pregnancy complications like preeclampsia (17). Our study shows that
243 *B. breve* improves pregnancy outcomes in mice, as indicated by the lower number of
244 resorptions, elevated placental efficiency and restored fetal glycaemia and weight. *B. breve*
245 UCC2003 was also shown to induce changes in the metabolite milieu, including acetate,
246 acetylcarnitine and carnitine in the mother and placenta, which were likely key for the
247 beneficial effects on fetal growth. Acetate is a major bifidobacterial fermentation by-product,
248 which directly mediates epithelial cell responses but also exerts systemic beneficial metabolic
249 effects (18, 19). More generally, microbial-derived short-chain fatty acids (SCFAs) modulate
250 multiple host physiological systems and during pregnancy are associated with maternal
251 gestational weight, neonatal length and body weight, and protection against allergic airway
252 disease in the developing fetus (20, 21). Acetate crosses the placenta (21), so in our model,
253 the elevated maternal *B. breve*-derived acetate may exert beneficial effects on feto-placental
254 growth via (i) maternal effects, through interactions within the maternal gut mucosa as
255 evidenced by higher maternal caecum acetate concentrations in *B. breve* supplemented (and
256 SPF dams vs. GF) and the subsequent impact on maternal organs (liver, adipose and spleen)
257 and nutrient handling, (ii) effects on the placenta, through use of acetate for cellular
258 metabolism, growth and function, and/or (iii) effects on the fetal metabolism following transport
259 of acetate across the placenta to the fetus. Compared to the maternal caecum, levels of
260 acetate were relatively low in the placental Lz and fetal liver (for all 3 groups). This suggests
261 that *B. breve* (and SPF microbiota-derived acetate) may be used to support anabolic
262 processes *in utero* (hence the very low levels detected), and together with changes in
263 acetylcarnitine and carnitine, may be supported by our observations of elevated fatty acid
264 transporter expression in the placenta and differentially regulated genes in the fetal liver. The
265 observed modulation of immune-associated pathways in the fetal liver, including those
266 associated with G protein-coupled receptor signalling (e.g. *Dusp9*), also indicates a role for
267 direct acetate-associated responses (22). *B. breve* supplementation also restored fetal
268 glycaemia and weight in BIF mice, achieving similar values to that seen for SPF fetuses.
269 Previous *in vivo* studies indicate different strains of *Bifidobacterium* (including *B. breve*)
270 modulate glucose handling (23), with this genus also consistently associated with potential
271 protection against human metabolic disorders e.g. type 2 diabetes (24, 25). In addition, our
272 observations of reduced maternal gonadal fat mass and maternal liver weight in *B. breve*-
273 treated dams compared to SPF dams, suggest that *Bifidobacterium,* or *B. breve* metabolites,

could affect maternal metabolic responses in key organs of the mother. In fact, previous work in adult mice suggests elevation of gut acetate levels due to *Bifidobacterium* treatment plays a key role in regulating glucose handling systemically and reduces visceral fat accumulation (26).

Maternal microbiota significantly affected the placental vascular bed by modifying the elongation of their fetal capillary network, which is required for adequate fetal growth (27). Moreover, *B. breve* significantly reduced the interhaemal membrane barrier thickness of the placenta, which may facilitate exchange of nutrients and gases. The mechanisms governing these structural changes could be partially mediated by changes in the expression of two imprinted genes (28), *Igf2* (namely the placenta-exclusive isoform, *Igf2P0*) and *Dlk1*, and via MAPK upregulation. In this regard, deletion of *Igf2P0* results in feto-placental growth restriction in association with reduced placental surface area for exchange, fetal capillary volume and increased barrier thickness (reviewed by (29)); parameters that were partially improved by *B breve* UCC2003 in line with the *Igf2P0* mRNA upregulation. Interestingly, *Igf2P0* is important for the structural and transport adaptations occurring in the placenta in response to maternal nutritional restriction (30) and recent work has shown that *Igf2* in the placenta interacts with MAPK signaling (31). *Dlk1,* a non-canonical ligand of the Notch signalling pathway localized to the endothelial cells of fetal capillaries in the placental Lz, also regulates placental vascularisation and branching morphogenesis (32). In addition, IGF2 and DLK1 can both mediate cellular actions via the MAPK pathway (33, 34). *Mapk14*, also known as p38MAPK, forms part of a signal transduction pathway that has been linked to environmental stresses and inflammatory cytokines (35). However, p38MAPK also regulates many normal cellular processes, including proliferation and cytoskeletal organisation. Furthermore, research in mice has demonstrated that *Mapk14* is essential for embryogenesis and placental Lz angiogenesis and vascular remodeling (36). In addition, placentas exposed to *B. breve* UCC2003, had lower concentrations of acetylcarnitine and carnitine compared to SPF, suggesting a greater reliance on these compounds for energy production, or enhanced transfer of these fatty acids to the fetus (37). Carnitine is well-known for mediating the transport of fatty acids into mitochondrial matrix for fatty acid β-oxidation. Carnitine can also promote p38MAPK signalling activation in cardiac tissue (38). Taken together, placental structural, transport and metabolic changes seen with *B. breve* UCC2003 treatment may link to the altered metabolites/nutrient milieu in the mother and would have been beneficial in providing additional substrates for fetal growth and development (when compared to GF; Figure S4).

While our study has clear strengths and strong translational implications for pregnancy complication treatments, it also has certain limitations. Unsurprisingly, we did not see a full ‘rescue’ of placental phenotype in the monocolonised GF *B. breve* (BIF) group, compared to complex microbiota found in SPF dams. However, structural and functional adaptations of

these placentas exposed to *B. breve* were adequate enough to 'rescue' fetal weight and fetal glycaemia. An array of gut-associated signaling and a diverse metabolite pool are expected to provide more complete placental development. Indeed, other or additional *Bifidobacterium* species and/or strains may be required for placental and fetal development, given strain-specific host physiology responses (16, 39). Further studies should allow the relative contributions of other microbial- and *Bifidobacterium*-derived factors to be elucidated. In addition, future work should evaluate the role of *B. breve* across gestation using larger cohorts of mice. Nonetheless, this study has revealed novel roles for *Bifidobacterium* and provides a safe therapeutic strategy for treating pregnancy complications, suggesting an opportunity for *in utero* programming through maternal *Bifidobacterium* and associated metabolites.

Overall, although our study was performed in mice and is not representative of a clinical scenario, our study highlights the importance of the maternal gut microbiota during gestation and demonstrates that *B. breve* modulates maternal physiology, placental structure and nutrient transporter capacity with impact on fetal glycaemia and fetal growth (Figure S4). Our findings prompt an in-depth investigation into how additional members of the gut microbiota impact on pregnancy outcomes. These future studies are important for the design of novel therapies to combat fetal growth restriction and other pregnancy complications.

Materials and Methods

***Bifidobacterium breve* UCC2003/pCheMC**

B. breve UCC2003/pCheMC was generated by introducing the plasmid pCheMC to electrocompetent *B. breve* UCC2003 as described previously (40). In brief, *B. breve* UCC2003 was grown until mid-log phase, chilled on ice and washed twice with ice cold sucrose citrate buffer (1mM citrate, 0.5M sucrose, pH5.8) and then electroporation of cells was carried out under the following conditions; 25 MF, 200 Ohms, 2 KV. Transformed cells were incubated for 2 hours in Reinforced Clostridial Medium (RCM) at 37ºC in a controlled anaerobic chamber then plated (41) on RCM agar plates with selective antibiotics. Colonies were sub-cultured 3 times on RCM agar plates with selective antibiotics. Antibiotics were used at the following final concentrations erythromycin 2µg/mL.

Lyophilised *B breve*

B. breve was grown in De Man, Rogosa and Sharpe agar (MRS) under anaerobic conditions overnight. The bacterial cell pellet was resuspended in 10% milk powder and lyophilised in 200 ml quantities. Lyophilised *B. breve* was reconstituted with 500µl PBS. Concentration of *B. breve* was 10^{10}CFU/ml. All batches were tested for contamination upon reconstitution on Luria-Bertani (LB) and Brain-Heart Infusion (BHI) plates under anaerobic and aerobic conditions at 37°C. No contamination of *B. breve* was detected.

352 **Mice**
353 All mouse experiments were performed under the UK Regulation of Animals (Scientific
354 Procedures) Act of 1986. The project license PDADA1B0C under which these studies were
355 carried out was approved by the UK Home Office and the UEA Ethical Review Committee. All
356 mice were housed in the Disease Modelling Unit at the University of East Anglia, UK. Animals
357 were housed in a 12:12 hour light/dark, temperature-controlled room and allowed food and
358 water ad libitum. Female Germ Free C57BL/6J (GF) and Specific Pathogen Free (SPF) mice
359 aged 6-8 weeks were used for the study. GF mice were bred in germ free isolators (2 females
360 to 1 male) and on gestational day (GD) GD9.5, pregnant mice (confirmed by weight) were
361 removed from the GF isolator and transferred to individually ventilated cages. The sterility of
362 these cages was previously tested and found to be suitable for housing GF mice for 1 week.
363 Sterile water was changed every 2 days.
364
365 ***B. breve* colonisation levels**
366 Mice were given 100µL of reconstituted lyophilised *B. breve* UCC2003 by oral gavage
367 (containing 10^{10} CFU/mL) at GD10, GD12 and GD14 or 100µL vehicle control (PBS, 4 %
368 skimmed milk powder), with this dosing regimen reflecting a more realistic time frame for
369 women who are more likely to start taking probiotics once their pregnancy is confirmed. At
370 GD16.5 and GD18.5, mice were sacrificed by cervical dislocation and samples collected for
371 molecular and histological analysis. The experimental design can be found in Figure S1.
372
373 Faecal samples were checked for contamination and *B. breve* colonization at GD12 and GD14
374 and GD16. Briefly, faecal samples from GF and GF treated with *B. breve* were diluted in 500
375 µL of PBS and agitated for 30 mins at 4˚C on an Eppendorf MixMate 5353 Digital Mixer Plate
376 Shaker. The faecal solution was passed through a 0.45µm syringe filter. Faecal solution was
377 diluted 1 in 100 and 20 µL was added to a De Man, Rogosa and Sharpe agar plate with
378 erythromycin and incubated for 48 hours in an anaerobic chamber at 37˚C. Colony forming
379 units were counted using a click counter.
380
381 **Blood hormones and circulating metabolites**
382 Maternal blood was obtained by cardiac exsanguination immediately after cervical dislocation.
383 Blood was centrifuged and serum collected and stored at -80ºC until further analysis. Blood
384 glucose and plasma concentrations of leptin, insulin, triglycerides, cholesterol, and free fatty
385 acids were determined as previously reported (42). Fetal blood glucose levels were measured
386 with a handheld glucometer (One Touch Ultra; LifeScan) immediately after decapitation of the
387 fetus.
388
389 **Placental histology**
390 Placentas were cut in half and fixed in 4% paraformaldehyde overnight at 4ºC. Samples were

391 washed 3 times with PBS for 15 minutes each and storage in 70% ethanol until embedding in
392 wax. Embedded placentas were cut at 5µm thickness and stained with haematoxylin and eosin
393 for gross morphology. Placental layer volumes were calculated using the Computer Assisted
394 Stereological Toolbox (CAST v2.0). For analysis of labyrinth components, sections were
395 stained with lectin for identification of fetal endothelial vessels and with cytokeratin for
396 trophoblasts. Further details of the double-labelling immunohistochemistry and the analysis
397 performed can be found elsewhere (43). For the analysis of placental glycogen, sections were
398 stained with Periodic acid–Schiff (Sigma-Aldrich) previous incubation with 0.5% periodic acid
399 (Thermo Fisher Scientific). Sections were counterstained with Fast-green (Sigma-Aldrich) and
400 digitalized with the nanozoomer scanner (Hamamatsu). Analysis of placental glycogen
401 accumulation was performed with Image J and conducted blinded to experimental groups.
402 TUNEL staining for placental cell death was performed using the TUNEL Assay Kit - HRP-DAB
403 (Abcam, ab206386) following manufacturer instructions except for the counterstaining which
404 was substituted for Nuclear Fast Red (Vector). Sections were digitalized using a nanozoomer
405 scanner (Hamamatsu) and the amount of apoptosis in the labyrinth zone was calculated in 5
406 random areas (x20 magnification) and analysed by Image J software.
407
408 **Western blotting**
409 Protein extraction was performed with RIPA buffer as described previously (44). Lysates were
410 separated by SDS-PAGE and incubated with antibodies against p-MAPK (Thr202/Tyr204)
411 (Cell Signalling, 4370; 1/1000), t-MAPK 44/42 (Cell Signalling, 4695; 1/1000), DLK-1 antibody
412 (Abcam, ab21682; 1/1000), p-P38MAPK (Cell Signalling, 4511; 1/1000) and t-P38MAPK (Cell
413 Signalling, 8690; 1/1000). Reactive bands were detected by chemiluminescence (Thermo
414 Scientific, Scientific SuperSignal West Femto) and quantified by Image J software. Proteins
415 were normalized to Ponceau S Staining (45).
416
417 **RNA extraction and qPCR**
418 Extraction of RNA from micro-dissected placental labyrinth zones was performed with RNeasy
419 Plus Mini Kit (Qiagen) and reverse transcribed using the High Capacity cDNA RT Kit minus RT
420 inhibitor (Applied Biosystems) according to manufacturer's instructions. Samples were
421 analysed using MESA Blue SYBR (Eurogentec) and primers (See Supplementary Table 3)
422 were synthesized by Sigma-Aldrich. The expression of each gene was normalized to the
423 geometric mean expression of two reference genes *Hprt* and *Ubc*, which remained stably
424 expressed across the groups. Analysis was performed using the 2-ΔΔCt method (46).
425
426 **Sequence pre-processing, Differential Gene Expression (DGE) analysis and Functional**
427 **enrichment analysis**
428 Fetal liver RNA on GD18.5 was extracted using the RNeasy Plus Mini Kit (Qiagen). RNA
429 sequence pre-processing and DGE analysis was performed as previously described with slight

430 modifications (14). Briefly, FASTQ reads were initially quality-filtered using fastp v0.20.0 with
431 options -q 10 (sequence reads with phred quality <10 were discarded). Subsequently,
432 sequence reads for each sample were merged (merge-paired-reads.sh) and followed by rRNA
433 sequence filtering via SortMeRNA v2.1 based on SILVA rRNA database optimised for
434 SortMeRNA software (47, 48). Filtered reads were then unmerged (unmerge-paired-reads.sh)
435 and ready for transcript quantification. Transcript mapping and quantification were then
436 performed using Kallisto v0.44.0 (49). *Mus musculus* (C57BL/6 mouse) cDNA sequences
437 (GRCm38.release-98_k31) retrieved from Ensembl database were indexed with Kallisto utility
438 *index* at default parameter and was used for following transcript mapping and abundance
439 quantification via Kallisto utility *quant* at 100 bootstrap replicates (-b 100) (50).
440
441 RNA raw counts were subjected (Kallisto outputs) to DGE analysis, which was performed
442 using R library *Sleuth* (v0.30.0) (51). Transcripts were then mapped to individual genes using
443 Ensembl BioMart database (GRCm38.p6) with function *sleuth_prep* and option *gene_mode =*
444 *TRUE*. Genes with an absolute $\log_2$ (fold change) >1.0 and q value <0.05 (p-adjusted value;
445 based on Wald test statistics) were considered to be differentially regulated (52). DGE
446 statistics were plotted via functions within package *Sleuth*. Finally, functional enrichment
447 analysis was performed using g:Profiler webtool g:GOst based on organism *Mus Musculus*
448 species (53). Briefly, a list of DGEs (Ensembl IDs) was uploaded to g:GOst, then selected 'GO
449 molecular function', 'GO biological process' and 'Reactome' in the 'data sources'. Significance
450 threshold was set at 0.001 (g:SCS threshold).
451
452 **Metabolite extraction, Nuclear Magnetic Resonance (NMR) spectroscopy and metabolite**
453 **quantification**
454 Extraction of metabolite from liver, placenta, caecum contents and culture (spent) media
455 samples were performed as previously described as a standard protocol (54). For caecal
456 samples, frozen materials (stored at -80°C prior to analysis) were weighed ~50 mg before the
457 addition of 600 µL of faecal water phosphate buffer solution. The faecal water phosphate buffer
458 was prepared as follows: add 0.51g $NaH_2PO_4.H_2O$ and 2.82g K_2HPO_4 to 200 mL D_2O
459 (Deuterium Oxide; Merck). To this, 34.5 mg TSP (Trimethylsilyl propanoic acid; used as NMR
460 standard) and 100 mg NaN_3 (Merck) were added (55). Next, the mixture was centrifuged for 10
461 min at 17,000 x g before transferring the mixture to an NMR tube (Merck) for subsequent NMR
462 analysis.
463
464 For liver and placenta samples (stored at -80°C prior to analysis), frozen fresh tissue (~20-45
465 mg) was placed into a 2 ml sterile microcentrifuge tube pre-loaded with ~15-20 glass beads
466 (Merck) while 200 µL of ice-cold methanol (Fisher Scientific) and 42.5 µL of ultra-pure cold
467 water were added to it and vortexed. Tissue was disrupted via a tissue lyser (Qiagen) for 2 x 2
468 mins. 100 µL of ice-cold chloroform (Merck) was then added and vortexed. 100 µL of ice-cold

469 chloroform and 100 µL of ultra-pure cold water were added to the mixture, and kept on ice for
470 15 min. Liquid was then transferred into a new sterile microcentrifuge tube and centrifuged for
471 3 min at 17,000 x g. The top aqueous phase was transferred into a new microcentrifuge tube
472 and speed-vacuumed for 30 min at 50°C and 30 min without heating prior to reconstitution with
473 faecal water phosphate buffer solution at 600 µL. The mixture was then moved to an NMR
474 tube (Merck) for subsequent NMR analysis. Metabolites from culture media Brain Heart
475 Infusion (BHI; Oxoid) and spent media (BHI cultured with *B. breve* UCC2003 for 48 h) were
476 extracted as follows: 400 µL of medium was transferred into a sterile microcentrifuge tube with
477 the addition of 200 µL faecal phosphate buffer and mixed well. The mixture was then moved to
478 an NMR tube (Merck) for further NMR analysis.
479
480 Samples in NMR tubes were subsequently subjected to NMR spectroscopy. The ^{1}H NMR
481 spectra were recorded at 600 MHz on a Bruker AVANCE spectrometer (Bruker BioSpin
482 GmbH, Germany) running Topspin 2.0 software. The metabolites were then quantified using
483 the software Chenomx® NMR Suite 7.0™.
484
485 **Statistical analysis**
486 All statistical analysis and sample size are shown in each figure/table and in the corresponding
487 figure/table legends. Only samples from viable fetuses were analysed. No statistical analysis
488 was used to pre-determine sample size and samples were assigned code numbers and
489 analysis was performed in a blinded fashion. Statistical calculations were performed using the
490 GraphPad Prism software (GraphPad, San Diego, CA), SAS/STAT (Statistical System Institute
491 Inc. Cary, NC, USA) and RStudio Version 1.4.1106 (RStudio Boston, MA) with R Version 4.0.3
492 (Vienna, Austria). Morphometric parameters of mother and number of viable/resorption per
493 litter were analysed by one-way ANOVA followed by Tukey post hoc test. Resorption rate was
494 calculated with a general linear model with total litter size as a covariate. Feto-placental
495 weights, placental stereological measurements and placental Lz gene expression levels were
496 analysed with a general linear mixed model, taking into account viable litter size as a covariate
497 and taking each fetus as a repeated measure. Differences between individual metabolites
498 between the three groups were tested with a Kruskal-Wallis test using the kruskal.test function
499 with correction for multiple comparisons applied using the Benjamini & Hochberg false
500 discovery rate method using the p.adjust function. Pairwise comparisons between the three
501 groups were carried out with a Dunn's test on individual metabolites significantly different after
502 correction for multiple comparisons using the dunnTest function in the FSA package. ROUT
503 test was used for identification of outlier values. A probability value of < 0.05 was considered
504 significantly different.
505
506 **Acknowledgments**

JL-T currently holds a Sir Henry Wellcome Postdoctoral Fellowship (220456/Z/20/Z) and previously a Newton International Fellowship from the Royal Society (NF170988 / RG90199). LJH is supported by Wellcome Trust Investigator Awards (100974/C/13/Z and 220876/Z/20/Z); the Biotechnology and Biological Sciences Research Council (BBSRC), Institute Strategic Programme Gut Microbes and Health (BB/R012490/1), and its constituent projects BBS/E/F/000PR10353 and BBS/E/F/000PR10356. ANS-P is supported by a Lister Institute of Preventative Medicine Research Prize (RG93692). Authors would like to thank Dr Ruben Bermejo-Poza (Complutense University of Madrid) for statistical advice and the Ferguson-Smith laboratory (University of Cambridge) for providing the DLK1 antibody.

Data availability

The fetal liver RNA-Seq raw sequencing data are deposited at the National Center for Biotechnology Information (NCBI) under BioProject PRJNA748000. Relevant data are within the manuscript and its Supporting Information files. Scripts for differential gene expression analysis can be accessed at GitHub, https://github.com/raymondkiu/Maternal-foetal-microbiota-paper/

References

1. R. Krajmalnik-Brown, Z.-E. Ilhan, D.-W. Kang, J. K. DiBaise, Effects of Gut Microbes on Nutrient Absorption and Energy Regulation. *Nutr Clin Pract* **27**, 201–214 (2012).
2. B. McDonald, K. D. McCoy, Maternal microbiota in pregnancy and early life. *Science* **365**, 984–985 (2019).
3. M. G. de Agüero, *et al.*, The maternal microbiota drives early postnatal innate immune development. *Science* **351**, 1296–1302 (2016).
4. O. Koren, *et al.*, Host remodeling of the gut microbiome and metabolic changes during pregnancy. *Cell* **150**, 470–480 (2012).
5. M. Nuriel-Ohayon, *et al.*, Progesterone Increases Bifidobacterium Relative Abundance during Late Pregnancy. *Cell Rep* **27**, 730-736.e3 (2019).
6. T. Napso, H. Yong, J. Lopez-Tello, A. N. Sferruzzi-Perri, The role of placental hormones in mediating maternal adaptations to support pregnancy and lactation. *Front. Physiol.* **9** (2018).
7. E. S. Lamousé-Smith, A. Tzeng, M. N. Starnbach, The intestinal flora is required to support antibody responses to systemic immunization in infant and germ free mice. *PLoS One* **6**, e27662 (2011).
8. E. A. Kennedy, K. Y. King, M. T. Baldridge, Mouse Microbiota Models: Comparing Germ-Free Mice and Antibiotics Treatment as Tools for Modifying Gut Bacteria. *Frontiers in Physiology* **9**, 1534 (2018).
9. J. Lu, *et al.*, Microbiota influence the development of the brain and behaviors in C57BL/6J mice. *PLoS One* **13**, e0201829 (2018).
10. A. M. Martin, *et al.*, The gut microbiome regulates host glucose homeostasis via peripheral serotonin. *PNAS* **116**, 19802–19804 (2019).
11. M. M. Faas, *et al.*, Microbiota Induced Changes in the Immune Response in Pregnant Mice. *Front Immunol* **10**, 2976 (2019).
12. K. Pokusaeva, G. F. Fitzgerald, D. van Sinderen, Carbohydrate metabolism in Bifidobacteria. *Genes Nutr* **6**, 285–306 (2011).

13. S. Fanning, *et al.*, Bifidobacterial surface-exopolysaccharide facilitates commensal-host interaction through immune modulation and pathogen protection. *PNAS* **109**, 2108–2113 (2012).
14. R. Kiu, *et al.*, Bifidobacterium breve UCC2003 Induces a Distinct Global Transcriptomic Program in Neonatal Murine Intestinal Epithelial Cells. *iScience* **23**, 101336 (2020).
15. M. J. Dalby, L. J. Hall, Recent advances in understanding the neonatal microbiome. *F1000Res* **9**, F1000 Faculty Rev-422 (2020).
16. K. R. Hughes, *et al.*, Bifidobacterium breve reduces apoptotic epithelial cell shedding in an exopolysaccharide and MyD88-dependent manner. *Open Biol* **7**, 160155 (2017).
17. T. Miao, *et al.*, Decrease in abundance of bacteria of the genus Bifidobacterium in gut microbiota may be related to pre-eclampsia progression in women from East China. *Food & Nutrition Research* (2021) https:/doi.org/10.29219/fnr.v65.5781 (July 5, 2021).
18. S. Fukuda, *et al.*, Bifidobacteria can protect from enteropathogenic infection through production of acetate. *Nature* **469**, 543–547 (2011).
19. M. A. González Hernández, E. E. Canfora, J. W. E. Jocken, E. E. Blaak, The Short-Chain Fatty Acid Acetate in Body Weight Control and Insulin Sensitivity. *Nutrients* **11**, 1943 (2019).
20. M. Priyadarshini, *et al.*, Maternal short-chain fatty acids are associated with metabolic parameters in mothers and newborns. *Transl Res* **164**, 153–157 (2014).
21. A. N. Thorburn, *et al.*, Evidence that asthma is a developmental origin disease influenced by maternal diet and bacterial metabolites. *Nat Commun* **6**, 7320 (2015).
22. C. H. Kim, Control of lymphocyte functions by gut microbiota-derived short-chain fatty acids. *Cell Mol Immunol* **18**, 1161–1171 (2021).
23. K. Kikuchi, M. Ben Othman, K. Sakamoto, Sterilized bifidobacteria suppressed fat accumulation and blood glucose level. *Biochem Biophys Res Commun* **501**, 1041–1047 (2018).
24. H. Wu, *et al.*, Metformin alters the gut microbiome of individuals with treatment-naive type 2 diabetes, contributing to the therapeutic effects of the drug. *Nat Med* **23**, 850–858 (2017).
25. A. Solito, *et al.*, Supplementation with Bifidobacterium breve BR03 and B632 strains improved insulin sensitivity in children and adolescents with obesity in a cross-over, randomized double-blind placebo-controlled trial. *Clinical Nutrition* **40**, 4585–4594 (2021).
26. R. Aoki, *et al.*, A proliferative probiotic Bifidobacterium strain in the gut ameliorates progression of metabolic disorders via microbiota modulation and acetate elevation. *Sci Rep* **7**, 43522 (2017).
27. J. López-Tello, *et al.*, Fetal and trophoblast PI3K p110α have distinct roles in regulating resource supply to the growing fetus in mice. *Elife* **8** (2019).
28. J. M. Frost, G. E. Moore, The Importance of Imprinting in the Human Placenta. *PLOS Genetics* **6**, e1001015 (2010).
29. A. N. Sferruzzi-Perri, I. Sandovici, M. Constancia, A. L. Fowden, Placental phenotype and the insulin-like growth factors: resource allocation to fetal growth. *J Physiol* **595**, 5057–5093 (2017).
30. A. N. Sferruzzi-Perri, *et al.*, Placental-specific Igf2 deficiency alters developmental adaptations to undernutrition in mice. *Endocrinology* **152**, 3202–3212 (2011).
31. I. Sandovici, *et al.*, “The Imprinted Igf2-Igf2r Axis is Critical for Matching Placental Microvasculature Expansion to Fetal Growth” (2021).
32. A. Yevtodiyenko, J. V. Schmidt, Dlk1 expression marks developing endothelium and sites of branching morphogenesis in the mouse embryo and placenta. *Developmental Dynamics* **235**, 1115–1123 (2006).
33. C.-C. Huang, *et al.*, Soluble delta-like 1 homolog (DLK1) stimulates angiogenesis through Notch1/Akt/eNOS signaling in endothelial cells. *Angiogenesis* **21**, 299–312 (2018).
34. K. Forbes, M. Westwood, P. N. Baker, J. D. Aplin, Insulin-like growth factor I and II regulate the life cycle of trophoblast in the developing human placenta. *American Journal of Physiology-Cell Physiology* **294**, C1313–C1322 (2008).

35. A. Cuenda, S. Rousseau, p38 MAP-Kinases pathway regulation, function and role in human diseases. *Biochimica et Biophysica Acta (BBA) - Molecular Cell Research* **1773**, 1358–1375 (2007).
36. J. S. Mudgett, *et al.*, Essential role for p38α mitogen-activated protein kinase in placental angiogenesis. *PNAS* **97**, 10454–10459 (2000).
37. A. N. Sferruzzi-Perri, J. S. Higgins, O. R. Vaughan, A. J. Murray, A. L. Fowden, Placental mitochondria adapt developmentally and in response to hypoxia to support fetal growth. *Proc. Natl. Acad. Sci. U.S.A.* **116**, 1621–1626 (2019).
38. Z. Fan, Y. Han, Y. Ye, C. Liu, H. Cai, l-carnitine preserves cardiac function by activating p38 MAPK/Nrf2 signalling in hearts exposed to irradiation. *European Journal of Pharmacology* **804**, 7–12 (2017).
39. L. Ruiz, S. Delgado, P. Ruas-Madiedo, B. Sánchez, A. Margolles, Bifidobacteria and Their Molecular Communication with the Immune System. *Front Microbiol* **8**, 2345 (2017).
40. A. Mazé, M. O'Connell-Motherway, G. F. Fitzgerald, J. Deutscher, D. van Sinderen, Identification and Characterization of a Fructose Phosphotransferase System in Bifidobacterium breve UCC2003. *Applied and Environmental Microbiology* **73**, 545 (2007).
41. M. Cronin, *et al.*, High Resolution In Vivo Bioluminescent Imaging for the Study of Bacterial Tumour Targeting. *PLOS ONE* **7**, e30940 (2012).
42. B. Musial, *et al.*, Proximity to Delivery Alters Insulin Sensitivity and Glucose Metabolism in Pregnant Mice. *Diabetes* **65**, 851–860 (2016).
43. K. De Clercq, J. Lopez-Tello, J. Vriens, A. N. Sferruzzi-Perri, Double-label immunohistochemistry to assess labyrinth structure of the mouse placenta with stereology. *Placenta* **94**, 44–47 (2020).
44. E. Salazar-Petres, D. P. Carvalho, J. Lopez-Tello, A. N. Sferruzzi-Perri, "Placental mitochondrial function, nutrient transporters, metabolic signalling and steroid metabolism relate to fetal size and sex in mice" (2021).
45. I. Romero-Calvo, *et al.*, Reversible Ponceau staining as a loading control alternative to actin in Western blots. *Anal Biochem* **401**, 318–320 (2010).
46. K. J. Livak, T. D. Schmittgen, Analysis of relative gene expression data using real-time quantitative PCR and the 2(-Delta Delta C(T)) Method. *Methods* **25**, 402–408 (2001).
47. S. Chen, Y. Zhou, Y. Chen, J. Gu, fastp: an ultra-fast all-in-one FASTQ preprocessor. *Bioinformatics* **34**, i884–i890 (2018).
48. E. Kopylova, L. Noé, H. Touzet, SortMeRNA: fast and accurate filtering of ribosomal RNAs in metatranscriptomic data. *Bioinformatics* **28**, 3211–3217 (2012).
49. N. L. Bray, H. Pimentel, P. Melsted, L. Pachter, Near-optimal probabilistic RNA-seq quantification. *Nat Biotechnol* **34**, 525–527 (2016).
50. D. R. Zerbino, *et al.*, Ensembl 2018. *Nucleic Acids Res* **46**, D754–D761 (2018).
51. H. Pimentel, N. L. Bray, S. Puente, P. Melsted, L. Pachter, Differential analysis of RNA-seq incorporating quantification uncertainty. *Nat Methods* **14**, 687–690 (2017).
52. R. J. Kinsella, *et al.*, Ensembl BioMarts: a hub for data retrieval across taxonomic space. *Database (Oxford)* **2011**, bar030 (2011).
53. U. Raudvere, *et al.*, g:Profiler: a web server for functional enrichment analysis and conversions of gene lists (2019 update). *Nucleic Acids Res* **47**, W191–W198 (2019).
54. G. Le Gall, Sample collection and preparation of biofluids and extracts for NMR spectroscopy. *Methods Mol Biol* **1277**, 15–28 (2015).
55. J. Wu, Y. An, J. Yao, Y. Wang, H. Tang, An optimised sample preparation method for NMR-based faecal metabonomic analysis. *Analyst* **135**, 1023–1030 (2010).

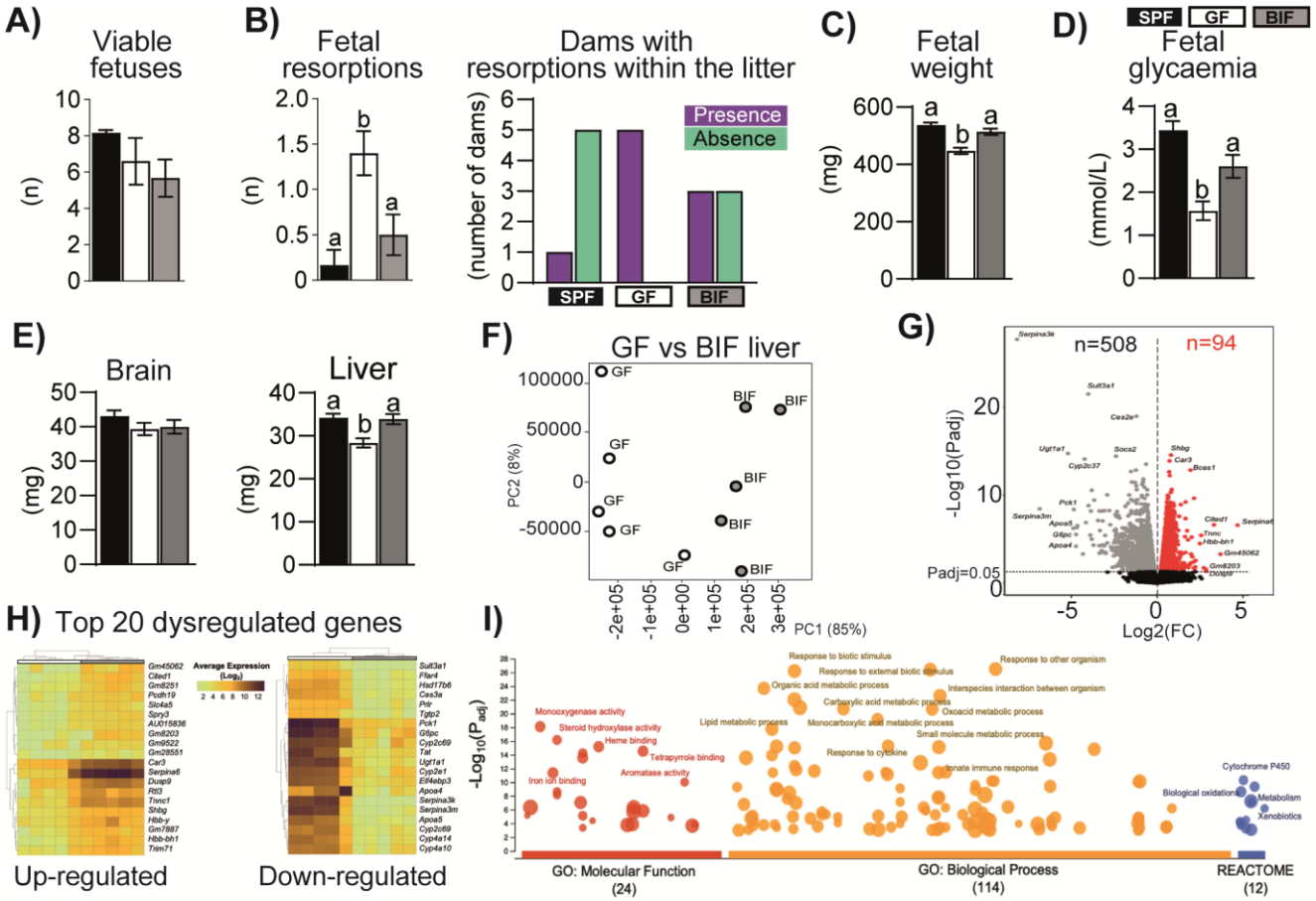

Figure 1. Effects of maternal gut microbiome and *B. breve* supplementation during pregnancy on fetal viability, growth and hepatic transcriptome. (A) Number of viable fetuses per litter, **(B)** Number of resorptions per litter (left) and number of dams with presence of resorptions within the litter (right), **(C)** Fetal weight, **(D)** Fetal blood glucose concentrations, **(E)** Fetal organ weights. All data shown in A to E were obtained on GD16.5 from: SPF (49 fetuses/6 dams), GF (33 fetuses/5 dams), BIF (34 fetuses/6 dams). **(F-I)** RNA-Seq analysis of fetal liver samples obtained at GD18.5, **(F)** PCA plot and **(G)** volcano plots showing up and down-regulated DEGs in BIF group (compared to GF group), **(H)** Heat map of the 20 most up and down-regulated DEGs (BIF group), **(I)** Functional profiling (g:Profiler) on 602 DEGs. Key enriched GO terms and REACTOME pathways are shown in the figure (significant threshold: P_{adj}<0.001). RNA-seq was performed on fetal livers obtained at GD18.5 from a total of 3 GF and 4 BIF pregnant dams/litters. Statistical analysis for data shown in **A-B** was performed by one-way ANOVA Tukey multiple comparisons test. Data in C-E was analysed with a general linear mixed model, taking into account litter size as a covariate and taking each fetus as a repeated measure followed by Tukey multiple comparisons test. RNA-Seq data analysis is described in the material and methods section. Different superscripts indicate significant differences between groups (a *versus* b and/or c: P<0.05; mean±SEM).

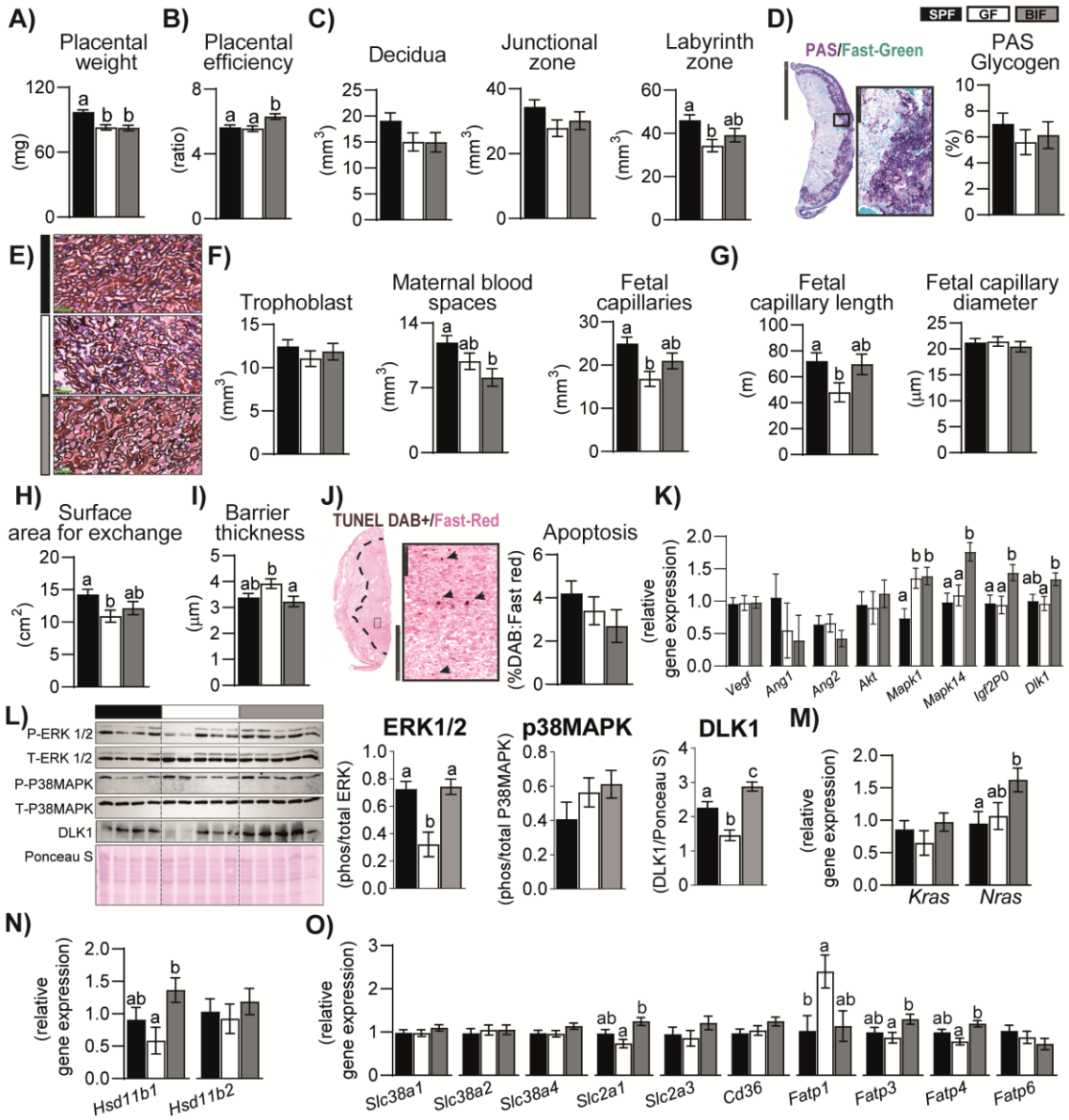

Figure 2. Effects of maternal gut microbiome and *B. breve* supplementation during pregnancy on placental structure and placental gene expression on GD16.5. (A) Placenta weight, **(B)** Placental efficiency determined by dividing fetal by placental mass, **(C)** Placental regional analysis, **(D)** Representative staining of placental glycogen with PAS and glycogen abundance, **(E)** Representative image of lectin and cytokeratin staining for labyrinth zone structural quantification, **(F-I)** Stereological parameters determined in placental labyrinth zone, **(J)** Representative image of TUNEL staining for apoptosis quantification in labyrinth zone **(K-O),** Gene expression levels in micro-dissected labyrinth. Data were analyzed by general linear mixed model, taking into account litter size as a covariate and taking each fetus as a repeated measure followed by Tukey multiple comparisons test. ROUT test was used for identification of outlier values. Different superscripts indicate significant differences between groups (a *versus* b: P<0.05; mean±SEM). Placental weight-efficiency was obtained from: SPF (49 fetuses/6 dams), GF (33 fetuses/5 dams), BIF (34 fetuses/6 dams). Laboratorial analysis was performed with: SPF (13-15 placentas/6 dams), GF (10-11 placentas/5 dams) and BIF (14-11 placentas/6 dams).

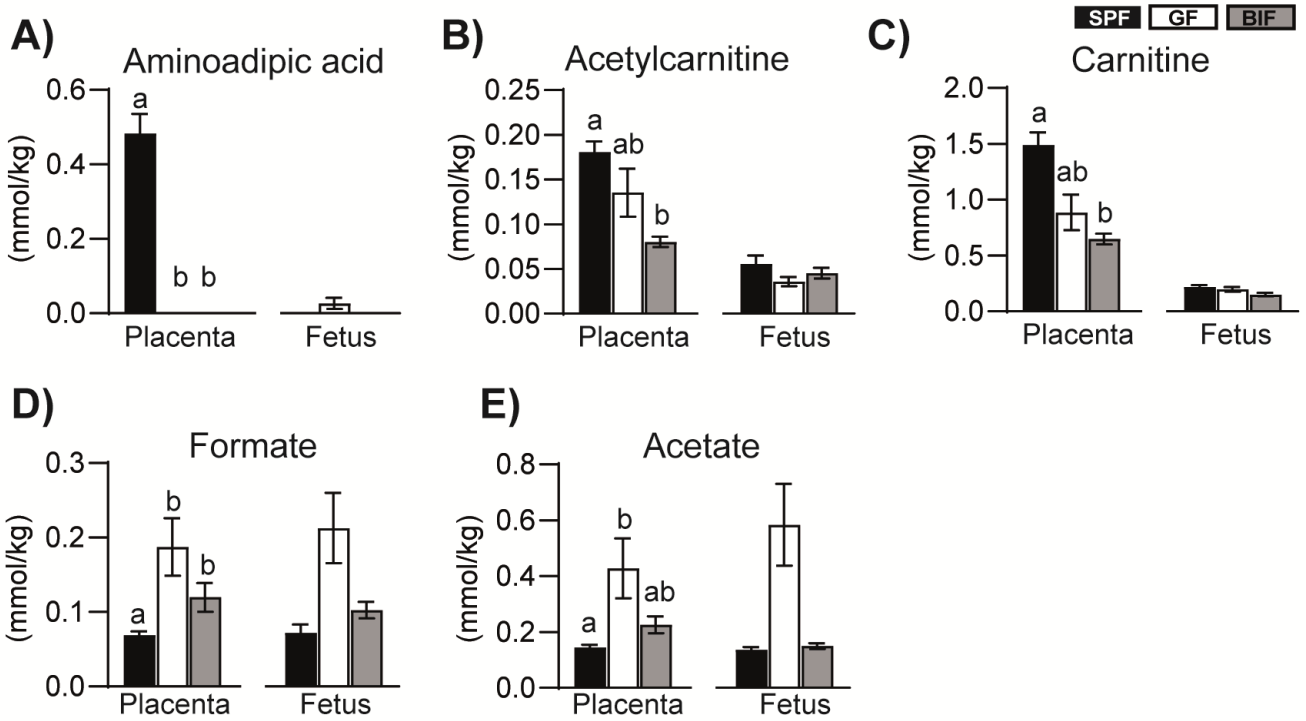

Figure 3. Metabolomic profiling of placental labyrinth zone and fetal liver on GD16.5. Data were analysed by Kruskal-Wallis test followed by multiple comparisons using the Benjamini & Hochberg false discovery rate method and Dunn's test. ROUT test was used for identification of outlier values. Different superscripts indicate significant differences between groups (a *versus* b, $P<0.05$). Data presented as mean±SEM. Number of placentas – livers analysed per group: SPF (8-8/4 dams), GF (6-8/4-5 dams), BIF (6-7/5 dams).

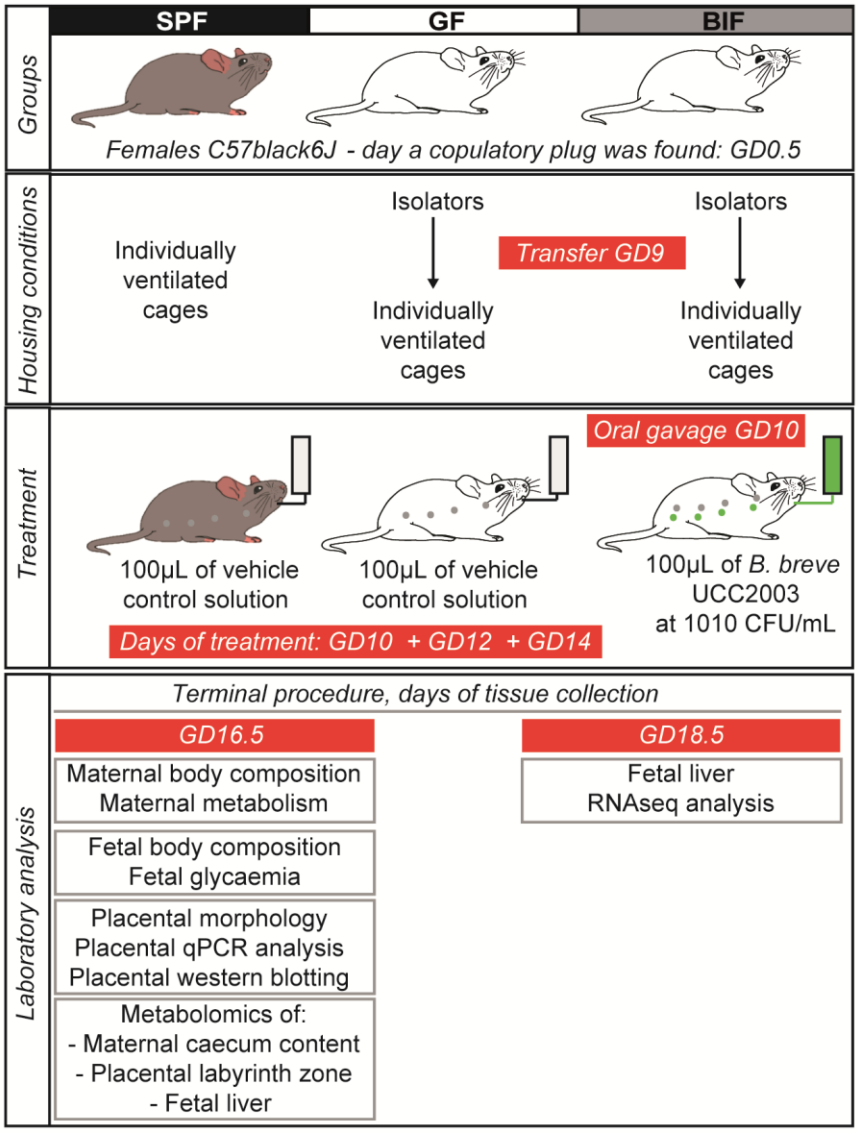

Supplementary Figure 1. Schematic representation of the experimental design. *B. breve* was administrated by oral gavage on gestational day (GD) 10, 12 and 14 to germ-free mice. Abbreviations: LZ (placental labyrinth zone); SPF (Specific-Pathogen-Free mouse); GF (Germ-Free mouse); BIF (Germ-Free mouse treated with *B. breve* UCC2003).

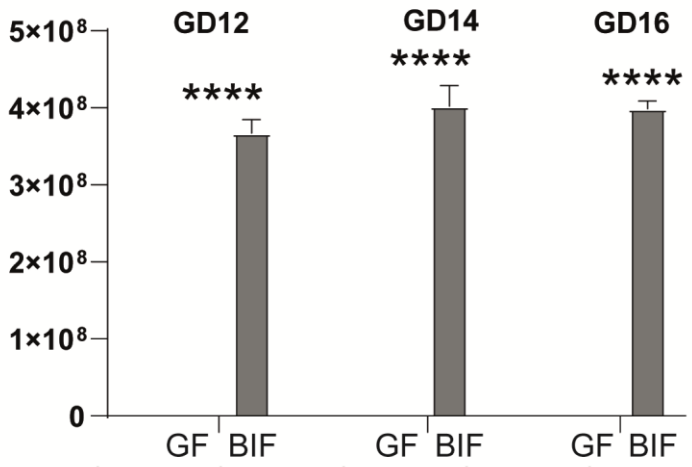

SPF group not analysed as cannot detect *B.breve* in SPF mice due to abundance of other bacteria

Supplementary Figure 2. Colonization levels of *B. breve* determined in maternal faecal samples on gestational day (GD), 12 and 14. Analysis performed by two-ways ANOVA (****P<0.0001). Data displayed as mean ± SEM. Number of dams for GF and BIF groups are 5 and 6, respectively.

Supplementary Figure 3. Resorption rate defined as the number of resorptions divided by the sum of resorptions and viable fetuses within the litter. Data displayed as mean ± SEM and analysed by general linear with total litter size as a covariate. Different superscripts indicate significant differences between groups.

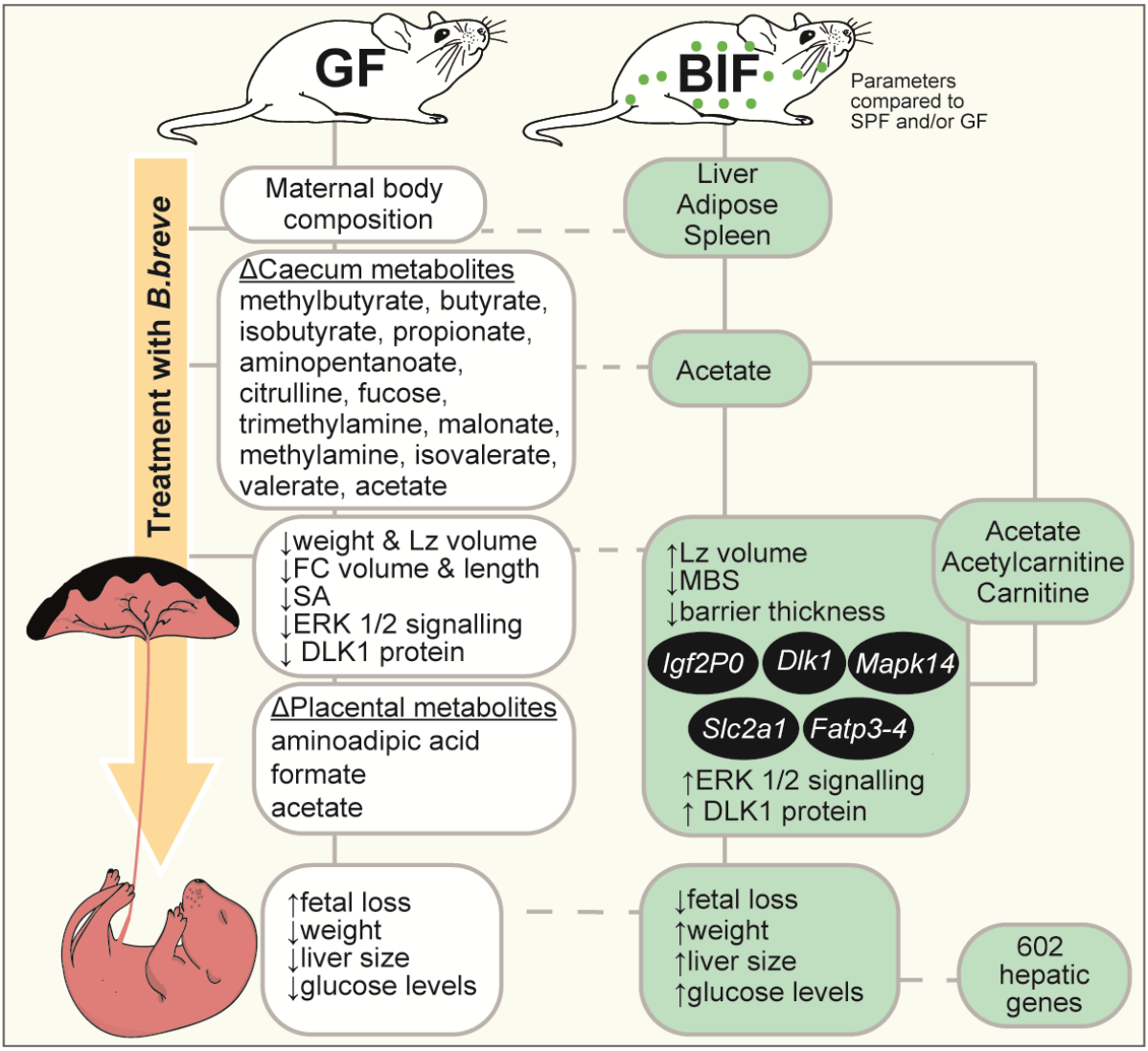

Supplementary Figure 4. Summary illustration showing how the maternal gut bacteria and *B. breve* affects mother, placenta and fetus during gestation. Abbreviations: LZ (placental labyrinth zone); SPF (Specific-Pathogen-Free mouse); GF (Germ-Free mouse); BIF (Germ-Free mouse treated with *B. breve* UCC2003); MBS (Maternal Blood Spaces); FC (Fetal Capillaries); SA (Surface Area).

Body composition				
	SPF (n=6)	GF (n=5)	BIF (n=6)	
Hysterectomy weight (g)	26.01±0.91	27.87±0.78	27.17±0.80	NS
Digestive Tract (g)	2.76±0.03[a]	6.83±0.32[b]	7.25±0.63[b]	****
Caecum (g)	0.66±0.03[a]	3.47±0.25[b]	3.96±0.41[b]	****
Small intestine (g)	1.66±0.03[a]	2.65±0.11[b]	2.59±0.14[b]	****
Pancreas (mg)	315.40±30.12[a]	183.40±24.74[b]	190.60±38.71[b]	*
Gonadal fat (mg)	433.10±43.20[a]	297.0±37.02[ab]	272.0±27.35[b]	*
Liver (g)	2.09±0.10[a]	1.79±0.05[ab]	1.55±0.08[b]	**
Spleen (mg)	117.90±2.80[a]	91.76±10.60[ab]	83.03±6.72[b]	*
Circulating metabolites and metabolic hormones				
	SPF (n=6)	GF (n=5)	BIF (n=6)	
Glucose (mmol/L)	8.08±0.78	8.38±1.18	8.88±0.74	NS
Insulin (µg/L)	0.12±0.004	0.19±0.05	0.20±0.06	NS
Leptin (pg/mL)	2465±177.1	2739±486	2425±303	NS
Cholesterol (mmol/L)	1.33±0.03	1.56±0.08	1.41±0.09	NS
Triglycerides (mmol/L)	1.54±0.08	1.79±0.14	1.50±0.11	NS
Free Fatty Acids (µmol/L)	890.6±101.3	1440±362	1092±114.5	NS
Caecum Metabolites				
	SPF (n=3)	GF (n=4)	BIF (n=4)	
2.Methylbutyrate (mmol/Kg)	0.05±0.01[a]	0±0.0[b]	0±0.0[b]	*
Isobutyrate (mmol/Kg)	0.41±0.24[a]	0±0.0[b]	0±0.0[b]	*
Butyrate (mmol/Kg)	12.48±7.97[a]	0±0.0[b]	0±0.0[b]	*
5.Aminopentanoate (mmol/Kg)	0.33±0.14[a]	0±0.0[b]	0±0.0[b]	*
Propionate (mmol/Kg)	4.48±1.99[a]	0±0.0[b]	0±0.0[b]	*
Citrulline (mmol/Kg)	0.30±0.07[a]	0±0.0[b]	0±0.0[b]	*
Fucose (mmol/Kg)	0.08±0.02[a]	0±0.0[b]	0±0.0[b]	*
Trimethylamine (mmol/Kg)	0.06±0.006[a]	0±0.0[b]	0±0.0[b]	*
Isovalerate (mmol/Kg)	0.09±0.01[a]	0±0.0[b]	0±0.0[b]	*
Methylamine (mmol/Kg)	0.05±0.02[a]	0±0.0[b]	0±0.0[b]	*
Malonate (mmol/Kg)	0.09±0.02[a]	0±0.0[b]	0±0.0[b]	*
Valerate (mmol/Kg)	0.57±0.27[a]	0±0.0[b]	0±0.0[b]	*
Acetate (mmol/Kg)	35.49±20.66[a]	0.55±0.06[b]	3.79±1.64[ab]	*

Table 1. Effects of maternal gut microbiome and *B. breve* administration during pregnancy on maternal body composition, circulating metabolites and hormones in maternal serum, and metabolites in caecum. Body composition and metabolites/hormones in serum were analyzed by one-way ANOVA followed by Tukey multiple comparisons test. Metabolites in maternal caecum were analysed by Kruskal-Wallis test followed by multiple comparisons using the Benjamini & Hochberg false discovery rate method and Dunn's test. ROUT test was used for identification of outlier values. Different superscripts indicate significant differences between groups (a *versus* b, P<0.05) (*P<0.05; **P<0.01; ***P<0.001;

743 ****P<0.0001; NS: not significant). Data presented as mean±SEM. The number of dams used
744 for each group is annotated on the table.

745 **Supplementary Table 1. List of differentially expressed genes and pathways detected in**
746 **the liver RNA-Seq on day 18.5 of gestation.**
747
748 **Supplementary Table 2. List of metabolites analysed in maternal caecum, placental**
749 **labyrinth zone and fetal liver on day 16.5 of gestation.**
750

751

	Forward	*Reverse*
Hprt	*CAGGCCAGACTTTGTTGGAT*	*TTGCGCTCATCTTAGGCTTT*
Ubc	*GGAGTCGCCCGAGGTCA*	*AAAGATCTGCATCGTCTCTCTCAC*
Vegf	*GAAGCTACTGCCGTCCGATT*	*CTTCATCGTTACAGCAGCC*
Ang1	*GAAGCAACTTCTCAACAGACA*	*TTCTTTGTGTTTTCCCTCCATT*
Ang2	*CTTCTACCTCGCTGGTGAAGAG*	*GCTAAAATCACTTCCTGGTTGG*
Akt	*GCCGCCTGATCAAGTTCTCC*	*TTCAGATGATCCATGCGGGG*
Mapk1	*TGCTTTCTCTCCCGCACAAA*	*GGCCAGAGCCTGTTCAACTT*
Mapk14	*AGCTGTCGAGACCGTTTCAG*	*GATGGGTCACCAGGTACACG*
Dlk1	*GAAAGGACTGCCAGCACAAG*	*CACAGAAGTTGCCTGAGAAGC*
Igf2P0	*GAGGAAGCTCTGCTGTTTGG*	*CAAAGAGATGAGAAGCACCAAC*
Hsd11b1	*GAGGAAGGTCTCCAGAAGGTA*	*ATGTCCAGTCCGCCCAT*
Hsd11b2	*GGCTGGATCGCGTTGTC*	*CGTGAAGCCCATGGCAT*
Slc38a1	*CGGCGCCTTTCCCTTTATTTC*	*CCGTTAACTCGAGGCCACTT*
Slc38a2	*TTCTGATTGTGGTGATTTGCAAGAA*	*CAGGATGGGCACAGCATACA*
Slc38a4	*AAGGTAGAGGCGGGAAAGGG*	*AGGAACTTCTGACTTTCGGCA*
Slc2a1	*GCTTATGGGCTTCTCCAAACT*	*GGTGACACCTCTCCCACATAC*
Slc2a3	*GA TCGGCTCTTTCCAGTTTG*	*CAA TCA TGCCACCAACAGAG*
Cd36	*ATGGGCTGTGATCGGAACTG*	*GTCTTCCCAATAAGCATGTCTCC*
Fatp1	*GGCTCCTGGAGCAGGAACA*	*ACGGAAGTCCCAGAAACCAA*
Fatp3	*GAGAACTTGCCACCGTATGC*	*GGCCCCTATATCTTGGTCCA*
Fatp4	*GATTCTCCCTGTTGCTCCTGT*	*CCATTGAAGCAAACAGCAGG*
Fatp6	*AACCAAGTGGTGACATCTCTGC*	*TCCATAAAGTAAAGCGGGTCAG*
Kras	*ACAGGCTCAGGAGTTAGCAAG*	*ACACAGCCAGGAGTCTTTTCT*
Nras	*CAAAGCAAGCCCACGAACTG*	*CATCGTCACTGCTGTTGAGC*

752 **Supplementary Table 3. List of primers used for placental labyrinth zone qPCR**